

284 Design and Development of a Six DOF Master-Slave Human-Assisted Manipulator Arm

Viboon SANGVERAPHUNSIRI, Tawee NGAMVILAIKORN
Faculty of Engineering, Chulalongkorn University, Bangkok, Thailand 10330

The development of a 6 DOF Master-Slave Human-Assisted Manipulator Arm with relaxation of kinematics similarity is purposed with experimental results. The Manipulator system consists of a Tendon-Pulley train Master-Arm and the 6 DOF, Chula III, slave arm with five-bar linkage. The maneuverability of the manipulator system is improved by using a virtual guidance and position gain (G_p). The virtual guidance, implement in the Master Arm, will improve the maneuverability for the operators, while the G_p will improve the accuracy of position and orientations of the system.

The experimental results shown that the operator with virtual guidance can control the slave arm very effective. The accuracy of positions and orientations will depends on the gain G_p , used for the path generation, which is the gain for amplifying the error signals of the master and slave system.

Keywords: Master-Slave, Human-Assisted Manipulator Arm, Virtual Guidance, Maneuverability

1. INTRODUCTION

Conventional robot arms are typically controlled by preprogramming of the desired paths within the robot workspace. Then the robot arms followed the desired programmed paths. There are some applications which we cannot form the desired paths at the beginning. The manual manipulation is needed to help the operator to control the manipulator arm. In this case the master-slave or tele-operation is required to fulfill the task. In this work we develop a 6 degree of freedom Master-Slave Human-Assisted manipulator arm with relaxation of kinematics similarity. We also introduce virtual guidance to improve the maneuverability for the operators. The virtual guidance can be a desired path or a boundary of the desired workspace. And any limited control volume can also be controlled or specified by virtual guidance technique.

Many Master arms have been developed in various configurations such as the Generalized Master Controller from University of California, Irvine. It is a 6 DOF with Pulley and cable with very rigid structure but contain many singularity points. The Master arm with JPL hand, from the California Institute of Technology and Jet Propulsion Lab, is based on the serial mechanism for the large working volume. It is very light. Due to the serial mechanism, the rigidity is low. Our Master arm is designed base on the serial link mechanism with reduction the effect of low rigidity structure in the operation motion direction.

2. THE MASTER-SLAVE SYSTEM

The master and slave arm as shown in the figure 1 are designed and built for this research by our laboratory. The master arm is a 6 DOF with Tendon-pulley train driving mechanism as shown in figure 2. The mechanism is back drive-able with zero backlash. The tendon-pulley system used in this mechanism has the same functions as the

pulley-belt shown in figure 3 with fixed or variable distance between the two unparallel rotating axes. As shown in figure 4, for the sliding-rotating link, we introduce a unique design of the tendon-pulley system which supports decouple motion of translation and rotation within the same driving mechanism. All the actuators are permanent magnet dc servo motors. They are located so that the inertia effect to the operator is minimized.



Figure 1. The Master-Slave Arm

The slave arm is a 6 DOF with five-bar linkage mechanism for the second and third joint as shown in figure 5. It is meant to be a high speed robot. The operating speed is five times faster than the typical commercial robots. The first three joints are actuated by the brushless dc servo motors. The other three joints are driven the permanent magnet dc servo motors. The force sensor can be installed at the wrist of the robot.

3. KINEMATICS

The forward kinematics of both the master and slave arm, the inverse kinematics of the slave arm, and the Jacobian of the master arm are required in the master-slave control system which will be discussed later. The master arm consists of 5 revolute joints and one prismatic joint at joint number 3. Using the Denavit-Hartenberg

and the coordinate system shown in figure 2, we can form the link parameters as shown in Table 1. The kinematics of the master and the slave arms are given below. More details of the analysis can be obtained from [7] and [8].

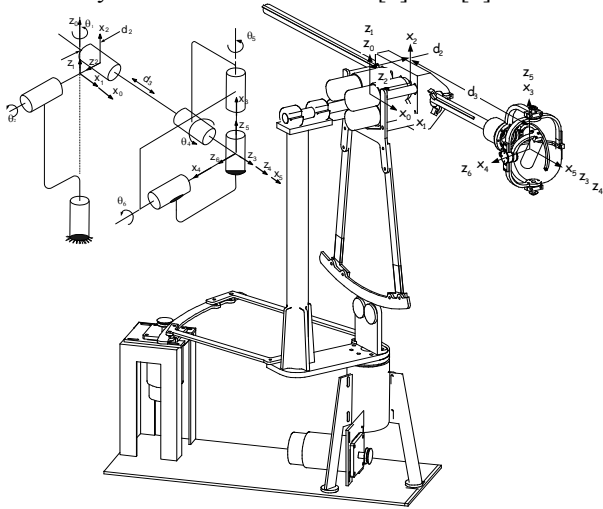


Figure 2. The Master Arm

i	α_{i-1}	a_{i-1}	d_i	θ_i
1	0°	0	0	θ_1
2	90°	0	$-d_2$	θ_2
3	90°	0	d_3	0
4	0	0	0	θ_4
5	90°	0	0	θ_5
6	90°	0	0	θ_6

Table 1 the link parameters of the master arm

The Forward Kinematics of the Master arm

The Transformation Matrix from frame 6 to frame 1 or the forward kinematics can be written below

$${}^0_6\mathbf{T} = \begin{bmatrix} r_{11} & r_{12} & r_{13} & p_x \\ r_{21} & r_{22} & r_{23} & p_y \\ r_{31} & r_{32} & r_{33} & p_z \\ 0 & 0 & 0 & 1 \end{bmatrix} \quad \text{where}$$

p_x, p_y, p_z = the end position with respect to the frame 0

and the $\begin{bmatrix} r_{11} & r_{12} & r_{13} \\ r_{21} & r_{22} & r_{23} \\ r_{31} & r_{32} & r_{33} \end{bmatrix}$ is the rotational matrix of the T (end

frame) frame with respect to the frame 0. The details of these components can be obtained from [7] and [8]

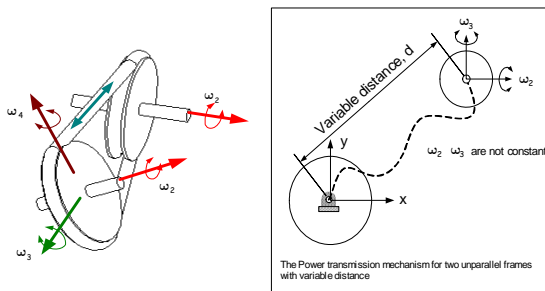


Figure 3. The Tendon-pulley system

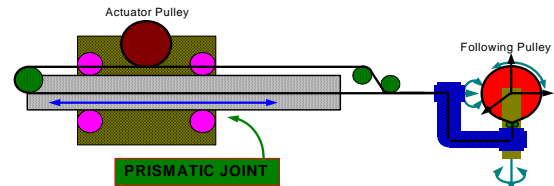


Figure 4. The Tendon-Pulley system of the sliding-rotating link

Jacobian of the Master Arm

For force and Torque control at the end point of the master arm, the torque at each joint of the master arm can be obtained from the transformation using the Jacobian as in the equation

$$\begin{bmatrix} \tau_1 \\ \tau_2 \\ \tau_3 \\ \tau_4 \\ \tau_5 \\ \tau_6 \end{bmatrix} = {}^6\mathbf{J}(\theta)^T \begin{bmatrix} f_x \\ f_y \\ f_z \\ m_x \\ m_y \\ m_z \end{bmatrix}$$

where τ = joint torque, f and m are external force and moment applied at the end point of the master arm. The detail of the Jacobian can be obtain from [7] and [8]

The Forward and Inverse Kinematics of the Slave Arm

The forward and inverse kinematics are necessary in the control loop of the slave arm. The master and slave are connected through the information of the end-effector. The inverse kinematics of the slave arm is used to convert the end-effectors to the joint angles of the slave arm. Figure 5 shows the configuration frame of the slave arm, the Chula III. The forward kinematics and the inverse kinematics of the slave arm will not show here. The details of the kinematics can be obtained from [7] and [8].

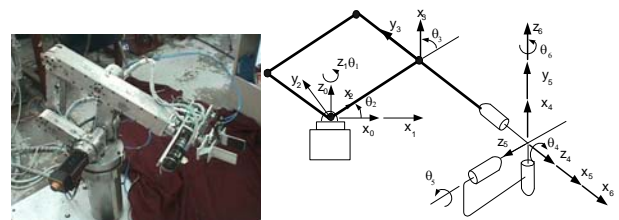
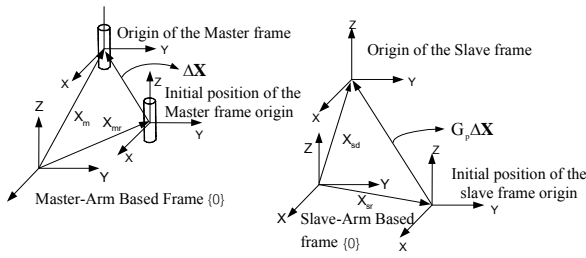


Figure 5. The Slave Arm

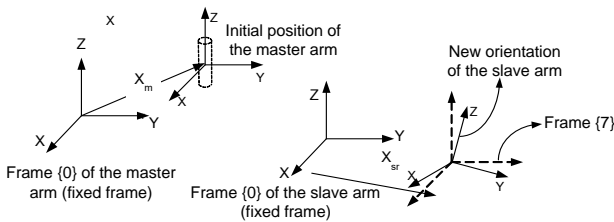
4. PATH GENERATION OF THE SLAVE ARM

Due to the different in configuration of the master and slave arm, the initial or home position of the master and slave arm have to be specified. In our case the home position of both arms are specified near the middle of their configuration based on read-out information of the sensors installed. So, the home position of the master arm and the slave arm are $p_x, p_y, p_z = [425 \ 10 \ 0]^T$, $[357 \ 0 \ 182]^T$ mm, respectively.



- \mathbf{X}_{sr} = the initial or home position of the slave arm
- \mathbf{X}_{mr} = the initial or home position of the master arm
- \mathbf{X}_{sd} = the desired end-effector position of the slave arm (operator control)
- \mathbf{X}_m = the end-effector position of the master arm
- \mathbf{X}_{md} = the desired end-position of the master arm

Figure 6. Link-frame Of The Master and Slave Arm (Translation).



- \mathbf{R}_{mr} = the initial orientation of the master arm
- \mathbf{R}_m = the orientation of the master arm
- \mathbf{R}_{md} = the desired orientation of the master arm (operator control)
- \mathbf{R}_{sr} = the initial orientation of the slave arm
- \mathbf{R}_{sd} = the desired orientation of the slave arm

Figure 7. Link-frame Of The Master and Slave Arm (Orientation).

As illustrated in Figure 6, when the operator control the master arm to any desired position, the translation position of the master arm can be evaluated from $\mathbf{X}_{md} = \mathbf{X}_{sr} + \Delta\mathbf{X}$ by using forward kinematics of the master arm. Where $\Delta\mathbf{X}$ is the different of the end-effector position from the initial position. Normally, the workspace of the slave arm are bigger than the workspace of the master arm. So, we will introduce an amplifier gain matrix G_p . The gain G_p is to amplifier the translation distance of the master arm to the slave arm distance as indicated in the equation $\mathbf{X}_{md} = \mathbf{X}_{sr} + G_p \Delta\mathbf{X}$. So, the desired position of the slave arm at any time is $\mathbf{X}_{sd} = \mathbf{X}_{md}$.

Due to the \mathbf{R} 's matrix are the 3x3 matrix, so, we can not use the vector algebra as being done in the translation case. By using Z-Y-Z Euler Angles representation, we can evaluate the desired rotation angles of each axis to obtain the desired orientation of the slave arm. From

$$\mathbf{R} = \begin{bmatrix} r_{11} & r_{12} & r_{13} \\ r_{21} & r_{22} & r_{23} \\ r_{31} & r_{32} & r_{33} \end{bmatrix},$$

the angle α, β, γ can be evaluated as following [6]:

if $\sin(\beta) \neq 0$, then

$$\beta = \arctan\left(\frac{\sqrt{r_{13}^2 + r_{32}^2}}{r_{33}}\right), \alpha = \arctan\left(\frac{r_{23}/\sin(\beta)}{r_{13}/\sin(\beta)}\right), \gamma = \arctan\left(\frac{r_{32}/\sin(\beta)}{-r_{31}/\sin(\beta)}\right)$$

where

$\alpha_{mr}, \beta_{mr}, \gamma_{mr}$ = Z-Y-Z Euler of \mathbf{R}_{mr}

$\alpha_m, \beta_m, \gamma_m$ = Z-Y-Z Euler of \mathbf{R}_m

$\alpha_{sr}, \beta_{sr}, \gamma_{sr}$ = Z-Y-Z Euler of \mathbf{R}_{sr}

$\alpha_{md}, \beta_{md}, \gamma_{md}$ = Z-Y-Z Euler of \mathbf{R}_{md}

$$\Delta\theta = \begin{bmatrix} \alpha_m - \alpha_{mr} \\ \beta_m - \beta_{mr} \\ \gamma_m - \gamma_{mr} \end{bmatrix} = \text{the rotation angle of the master arm}$$

The relation between the Z-Y-Z Euler angle of the \mathbf{R}_{md} and \mathbf{R}_{sr} can be written as

$$\begin{bmatrix} \alpha_{md} \\ \beta_{md} \\ \gamma_{md} \end{bmatrix} = \begin{bmatrix} \alpha_{sr} \\ \beta_{sr} \\ \gamma_{sr} \end{bmatrix} + G_p \Delta\theta$$

where G_p is the gain to amplifier the orientation distance of the master arm to the slave arm. From the Z-Y-Z Euler angle, $[\alpha_{md} \ \beta_{md} \ \gamma_{md}]^T$, the orientation matrix, \mathbf{R}_{md} , can be evaluated from

$$\mathbf{R}_{md} = \begin{bmatrix} c\alpha c\beta c\gamma - s\alpha s\gamma & -c\alpha c\beta s\gamma - s\alpha c\gamma & c\alpha s\beta \\ s\alpha c\beta c\gamma - c\alpha s\gamma & -s\alpha c\beta s\gamma - c\alpha c\gamma & s\alpha s\beta \\ -s\beta c\gamma & s\beta s\gamma & c\beta \end{bmatrix}$$

and finally $\mathbf{R}_{sd} = \mathbf{R}_{md}$.

5. VIRTUAL WALL

The concept of virtual wall is to specify the working area of the master arm virtually. This will help the operator to work in the specific area more convenience. Figure 8 shows the circular working area. The virtual wall is defined by a function, $f(x,y,z) = \text{constant}$. When the operator move the master arm contact to the virtual wall, the reaction force, F , will be generated to against the operation motion.

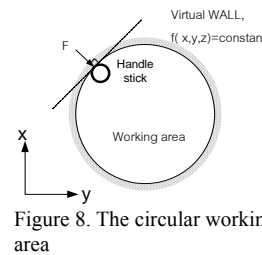


Figure 8. The circular working area

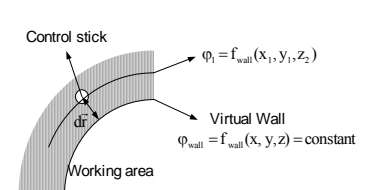


Figure 9. The Control Stick Are Beyond The Virtual Wall

From figure 9, the force F can be evaluated from

$$F = (K_1 dr) \vec{n} + (K_2 V) \vec{n}$$

where

$dr = \frac{d\phi |\nabla\phi|}{\nabla\phi \cdot \nabla\phi}$ = the distance between the control stick and the virtual wall

$\vec{n} = \pm \frac{\nabla\phi}{|\nabla\phi|}$ = the unit normal vector to the virtual wall

$$\nabla\phi = i \frac{\partial\phi}{\partial x} + j \frac{\partial\phi}{\partial y} + k \frac{\partial\phi}{\partial z}$$

V = velocity of the control stick

$(K_1 dr) \bar{n}$ = reaction force normal to the wall

$(K_2 V) \bar{n}$ = viscous force generated by the controller

K_1, K_2 = amplifier gains

So, the force F can be written as

$$F = \frac{K_1 d\phi}{|\nabla\phi|^2} \nabla\phi + K_2 V \frac{\nabla\phi}{|\nabla\phi|}$$

where

$$\begin{aligned} d\phi &= f_{wall}(x_1, y_1, z_1) - f_{wall}(x, y, z) \\ &= f_{wall}(x_1, y_1, z_1) - \phi_{wall} \\ &= f_{wall}(x_1, y_1, z_1) - \text{const} \end{aligned}$$

6. THE CONTROLLER

Figure 10 is the diagram to show the master-slave control system. The operator will control or maneuver the master arm through the control stick. The virtual wall will be specified in advance if necessary. When the control stick hits the virtual wall, the reaction force F , which reacts to the operator, will be generated by the controller in the cartesian space. The reaction force consists of 2 components, the force normal to the virtual wall and the viscous force generated by the controller to prevent the control stick move to fast. The reaction force F , in cartesian space, can be transformed into the joint space using the Jacobian matrix. The friction force compensation is also included in the control system as shown in the figure 10. When the control stick is inside the working area or in the free area, the reaction force applied at the control stick will only consist of the viscous force and friction compensation force.

The information from the encoders at each joint of the master arm will be used to calculate the desired path motion, translation and orientation, of the slave arm as mention in section 4. Then the joint angles of each links of the slave arm can be calculated by using the inverse kinematics. The PID control is used in the control loop of the slave arm as shown in figure 10. Then, the position and orientation error of the slave arm are obtained from the comparison of the measurement values with the input or the reference values.

7. EXPERIMENTAL RESULTS

The experiment covers both the general motion inside the working area without the boundary and the motion limited by the virtual wall or boundary. The general motion is done by setting $G_p = 0.5, 1.0, 2.0$ and 3.0 . And the slave arm is carrying a 2 kg. object. When the gain G_p is less than one, the slave arm will move slower than the master arm and vice versa. This paper will show only some examples of the graphical results from the experiments. More details of the experiment are described in [7] and [8].

Figure 11 shows an example of the comparison of the end-effector position of the master and slave arm when G_p is 0.5. The various G_p has been tried and the

results indicated that the maximum error in translation and orientation are less than 5 mm and 5 degrees, respectively.

For the motion with virtual boundary, the boundaries used in the experiment are a cylinder with 20 mm. in diameter and a circle with 40 mm. in diameter and $z = 160$ mm. The gain G_p in this case is set equal to 1.

Figure 12 shows the comparison of the end-effector position of the master and slave arm when boundary is cylinder with 20 mm in diameter. And Figure 13 shows the comparison of the end-effector position of the master and slave arm when the boundary is a circle with 40 mm. in diameter and $z = 160$ mm. Both experiments show that the initial position is beyond the boundary. This will cause the controller to generate the reaction force to bring the master arm inside the work area boundary.

The experimental results shown that the operator with virtual guidance can control the slave arm very effective. The accuracy of positions and orientations will depends on the gain G_p , used for the path generation, which is the gain for amplifying the error signals of the master and slave system.

8. CONCLUSION

This work is to develop a 6 DOF master-slave human-assisted manipulator arm with relaxation of kinematics similarity. The manipulator system consists of a Tendon-Pulley train Master-Arm and the 6 DOF, Chula III, slave arm with five-bar linkage. We introduce a unique design of the tendon-pulley system which supports decouple motion of the translation and rotation within the same driving mechanism. The maneuverability of the manipulator system is improved by using a virtual guidance and position gain G_p . The virtual guidance or virtual wall, implement in the master arm, will improve the maneuverability for the operators, while the G_p will improve the accuracy of position and orientations of the system.

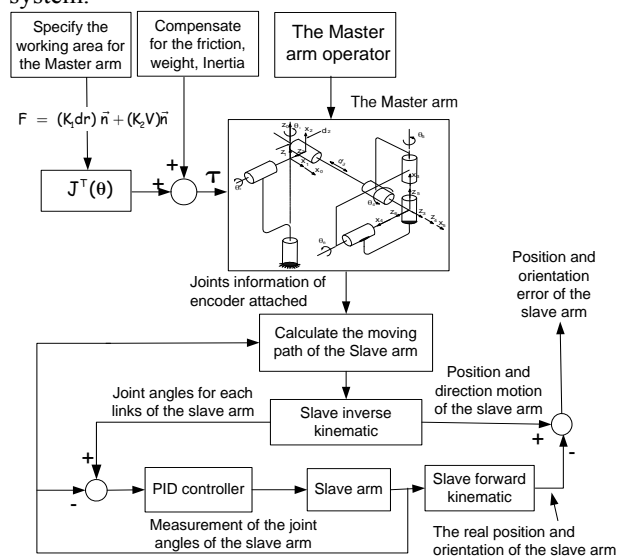


Figure 10. The Master-Slave Control System

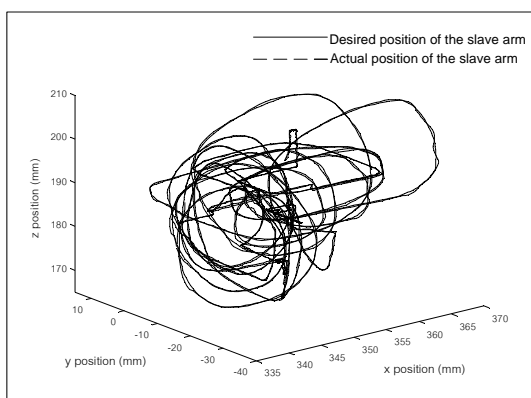


Figure 11. Comparison of the end-effector position of the master and slave arm when $G_p = 1$

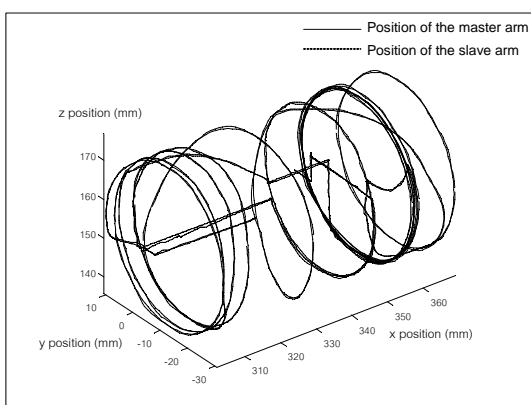


Figure 12. Comparison of the end-effector position of the master and slave arm when boundary is cylinder with 20 mm in diameter.

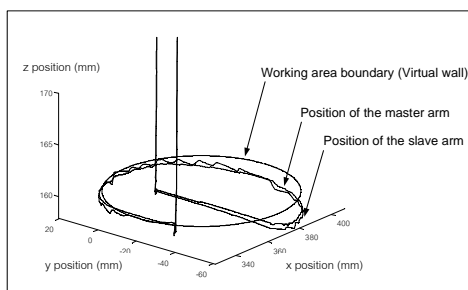


Figure 13. Comparison of the end-effector position of the master and slave arm when the boundary is a circle with 40 mm. in diameter and $z = 160$ mm.

REFERENCES

- [1] Gregory L. Long and Curtis L. Collins. A Pantograph linkage Parallel Platform Master Hand Controller. Proceeding of the 1992 IEEE.
- [2] Paul A. Millman and J. Edward Colgate. Design of four degree-of-freedom force-reflecting manipulandum with a specified force/torque workspace. Proceeding of the 1991 IEEE.
- [3] Nobuto Matsuhira, Makoto Asakura, Hiroyuki Bamba and Michihiro Uenohara. Development of an Advanced Master-Slave Manipulator Using a Pantograph Master Arm and a Redundant Slave Arm. Proceeding of the 1993 IEEE.
- [4] J.F. Jansen, R. L. Kress and S. M. Babcock. Controller Design for a force Reflecting Teleoperator System With Kinematically Dissimilar Master and Slave.
- [5] Paul S. Schenker, Antal K. Bejczy, Won S. Kim, Sukhan Lee. Advanced Man-Machine Interfaces and Control Architecture for Dexterous Teleoperation.
- [6] Craig J.J. Introduction to Robotic, Mechanics and Control, 2nd Edition: Addison Wesley Publishing Company, Inc., 1989.
- [7] Tawee Karmwilaikorn, Design and Development of a Master arm for Force-Reflecting system, Master Thesis, Department of Mechanical Engineering, Chulalongkorn University, April 2002.
- [8] Viboon Sangveraphunsiri, Tawee Karmwilaikorn, Development of a Six Degree-of-Freedom Master-Slave Manipulator System, Proceeding of the 15th Thailand Mechanical Engineering Network, Nov, 2001.